The emerging spectrum of cardiopulmonary pathology of the coronavirus disease 2019 (COVID-19): Report of 3 autopsies from Houston, Texas, and review of autopsy findings from other United States cities

Louis Maximilian Buja[a,*], Dwayne A. Wolf[b], Bihong Zhao[a], Bindu Akkanti[d,f], Michelle McDonald[a], Laura Lelenwa[a], Noah Reilly[a], Giulia Ottaviani[g], M. Tarek Elghetany[h], Daniel Ocazionez Trujillo[c], Gabriel M. Aisenberg[d,e], Mohammad Madjid[d], Biswajit Kar[d,f]

[a] Departments of Pathology and Laboratory Medicine, The University of Texas Health Science Center at Houston (UTHealth), Houston, Texas, USA
[b] Harris County Institute of Forensic Sciences, Houston, Texas, USA
[c] Diagnostic and Interventional Imaging, The University of Texas Health Science Center at Houston (UTHealth), Houston, Texas, USA
[d] Internal Medicine, McGovern Medical School, The University of Texas Health Science Center at Houston (UTHealth), Houston, Texas, USA
[e] Lyndon B. Johnson General Hospital, Harris Health, Houston, Texas, USA
[f] Center for Advanced Cardiopulmonary Therapies and Transplantation, McGovern Medical School and Memorial Hermann Hospital-Texas Medical Center, Houston, Texas, USA
[g] "Lino Rossi" Research Center for the Study and Prevention of Unexpected Perinatal Death and Sudden Infant Death Syndrome, Department of Biomedical, Surgical and Dental Sciences, University of Milan, Milan, Italy
[h] Department of Pathology, Baylor College of Medicine and Texas Childrens Hospital, Houston, Texas, USA

A R T I C L E   I N F O

A B S T R A C T

This paper collates the pathological findings from initial published autopsy reports on 23 patients with coronavirus disease 2019 (COVID-19) from 5 centers in the United States of America, including 3 cases from Houston, Texas. Findings confirm that COVID-19 is a systemic disease with major involvement of the lungs and heart. Acute COVID-19 pneumonia has features of a distinctive acute interstitial pneumonia with a diffuse alveolar damage component, coupled with microvascular involvement with intra- and extravascular fibrin deposition and intravascular trapping of neutrophils, and, frequently, with formation of microthombi in arterioles. Major pulmonary thromboemboli with pulmonary infarcts and/or hemorrhage occurred in 5 of the 23 patients. Two of the Houston cases had interstitial pneumonia with diffuse alveolar damage pattern. One of the Houston cases had multiple bilateral segmental pulmonary thromboemboli with infarcts and hemorrhages coupled with, in nonhemorrhagic areas, a distinctive interstitial lymphocytic pneumonitis with intra-alveolar fibrin deposits and no hyaline membranes, possibly representing a transition form to acute fibrinous and organizing pneumonia. Multifocal acute injury of cardiac myocytes was frequently observed. Lymphocytic myocarditis was reported in 1 case. In addition to major pulmonary pathology, the 3 Houston cases had evidence of lymphocytic pericarditis, multifocal acute injury of cardiomyocytes without inflammatory cellular infiltrates, depletion of splenic white pulp, focal hepatocellular degeneration and rare glomerular capillary thrombosis. Each had evidence of chronic cardiac disease: hypertensive left ventricular hypertrophy (420 g heart), dilated cardiomyopathy (1070 g heart), and hypertrophic cardiomyopathy (670 g heart). All 3 subjects were obese (BMIs of 33.8, 51.65, and 35.2 Kg/m^2). Overall, the autopsy findings support the concept that the pathogenesis of severe COVID-19 disease involves direct viral-induced injury of multiple organs, including heart and lungs, coupled with the consequences of a procoagulant state with coagulopathy.

* Corresponding author. Department of Pathology and Laboratory Medicine, McGovern Medical School, The University of Texas Health Science Center at Houston (UTHealth), 6431 Fannin St. MSB 2.276, Houston, Texas 77030, USA
E-mail address: l.maximilian.buja@uth.tmc.edu (L.M. Buja).

1. Introduction

A pneumonia of unknown cause was detected in Wuhan, China and was first reported to the World Health Organization (WHO) Country Office in China on 31 December 2019 [1]. The outbreak was identified as a Public Health Emergency of International Concern on 30 January 2020 and was declared a pandemic on March 11, 2020 [2]. On 11 February 2020, World Health Organization announced a name for the new coronavirus disease: coronavirus disease 2019 (COVID-19). The causative virus was identified and designated as SARS-CoV-2. [3,4]. Clinical reports from China have established that COVID-19 presents as an acute febrile respiratory illness as the dominant feature of a systemic disease involving multiple organ systems [5,6].

As the pandemic spread resulting in major morbidity and mortality, it became crystal clear to medically oriented pathologists, forensic pathologists and allied pulmonologists, cardiologists, and critical care physicians that autopsy of deceased victims of the disease was of paramount importance for gaining knowledge of its pathogenesis and pathophysiology. In a letter to the editor of Chest et al. raised a call to action, specifically for as many autopsies to be done as soon as possible to determine the pathologic substrate of this disease [7]. This is based on the well documented importance of the autopsy in establishing the etiology, pathogenesis, and response to treatment of emerging diseases [8].

However, pronouncements by regulatory agencies in the United States of America have led to confusion, delay and, all too often, suppression of the performance of autopsies at many institutions. Specifically, the Occupational Safety and Health Administration (OSHA) initially issued a contradictory statement with 1 sentence recommending suspension of postmortem procedures in suspected or confirmed COVID-19 cases and a second sentence indicating that, if deemed necessary and appropriate, strict adherence to basic safety procedures be used while performing such autopsies. In a subsequent statement from OSHA the first sentence was dropped [9]. The Centers for Disease Control (CDC) issued extensive guidelines which included rigorous standards for morgues and autopsy facilities to be under negative pressure with specific standards for venting the air from the rooms [10]. There followed a spectrum of administrative responses to the OSHA and Centers for Disease Control directives. But the overall effect has been to create more than necessary impediments for the task before us. Of note and particular relevance for the autopsy situation, Dr. Patricia Harris, President of the American Medical Association, has issued an important statement defending science in a time of fear and uncertainty [11].

Fortunately for scientific inquiry, several healthcare institutions and medical examiner jurisdictions have persisted in performing autopsies on suspected and confirmed COVID-19 cases. Just as a spectrum of responses has occurred for hospital autopsies, the same applies to medical examiner autopsies. Medical death investigation in the United States of America is a local function. It varies from state to state and from county to county. There are statewide, county, and regional systems that have substantial differences in their medicolegal jurisdiction. These considerations will determine the extent of COVID-19 autopsies in medical examiner jurisdictions around the country. A great service has been done by Dr. Alex Williamson of the Northwell Health System who has organized an autopsy working group and listserv for the sharing of information (awilliamson@northwell.edu).

Despite the challenges, autopsy studies are being performed and beginning to be reported from several locations around the United States of America, including Houston, Texas. The purposes of this paper are to collate and summarize the findings from these autopsy studies, including our own 3 initial cases, to correlate them with emerging clinical information, and to provide thoughts about how this information may help with designing treatment strategies. Correlation with information emerging from China, Europe and other countries also is touched upon.

2. Early reports from China

Liu et al. reported on an 85-year-old Chinese male who died following COVID-19 infection [12]. The report was limited to gross autopsy findings of heavy lungs with copious amounts of gray-white viscous fluid and unremarkable heart, liver and kidneys. Xu et al. performed postmortem sampling ("biopsies") of tissue from a 50-year-old man who died as a result of COVID-19 infection [13]. Both lungs demonstrated changes consistent with diffuse alveolar damage (DAD), the pathological correlate of acute respiratory distress syndrome (ARDS). The lungs showed interstitial lymphocytic infiltrates and atypical large pneumocytes with cytopathic changes consistent with a viral etiology. A few interstitial mononuclear inflammatory infiltrates were present in the heart and the liver showed moderate microvesicular steatosis.

Tian et al. reported findings on 2 patients who underwent lung lobectomies for adenocarcinoma and were retrospectively found to have had COVID-19 infection at the time of surgery [14]. On computed tomography (CT) scan, both patients exhibited bilateral ground glass opacities in the peripheral regions of the lungs. Histopathologically, the lungs of both patients exhibited edema, proteinaceous exudate, focal hyperplasia of pneumocytes, patchy inflammatory cellular infiltration, some multinucleated giant cells, and focal intra-alveolar fibrin deposits. Since neither patient had symptoms of pneumonia at the time of surgery, Tian et al. proposed that the changes likely represent an early phase of the lung pathology of COVID-19 pneumonia [14].

3. Findings from initial autopsy series in the United States of America (TABLES 1 and 2)

Two cases have been reported from the Office of the Chief Medical Examiner, Oklahoma City, OK [15]. The decedents were a 77-year-old obese man and a 42-year-old obese man both of whom had positive postmortem nasopharyngeal swab tests for SARS-CoV-2. The first patient had a history of hypertension, splenectomy and 6 days of fever and chills. The second patient was obese, had a history of myotonic dystrophy and developed abdominal pain followed by fever, shortness of breath and cough. Both of the deceased died outside of the hospital, and the autopsies showed evidence of emergency medical intervention, including intubation and chest compressions. Combined weight of the lungs was 2452 g for the first case and 1191 g for the second case. On histopathology, the lungs of the first case showed evidence of "DAD in the acute stage characterized by numerous hyaline membranes without evidence of interstitial organization. There was very patchy and sparse interstitial chronic/lymphocytic inflammation, and chronic inflammation and edema in the bronchial mucosa. A few small thrombi were noted within a few small pulmonary artery branches." Focal acute cardiomyocyte damage labeled as ischemic injury was found. Pulmonary pathology of the second case was dominated by acute bronchopneumonia with evidence of aspiration. Neither autopsy revealed viral inclusions, mucus plugging in airways, eosinophils, or myocarditis. The first case had a 402 g heart, marked 2 vessel coronary artery disease, and microscopic evidence of acute ischemic injury. The second case had a 372 g heart with no evidence of coronary artery disease or myocardial damage. The brains were reported as showing no gross abnormalities.

Four cases have been reported from the Department of Pathology of LSU Health Sciences Center, New Orleans, LA [16]. "The four decedents included male and female patients, ages 44–76. All were African American, and had histories of obesity class 2–3, and hypertension, controlled by medication. Three of the patients had

insulin-dependent type II diabetes, 2 had known chronic kidney disease (stages 2 and 3) and 1 was taking methotrexate. In all cases the clinical course consisted of approximately 3 days of mild cough and fever, with sudden respiratory decompensation just prior to arrival in the emergency department. Chest radiographs revealed bilateral ground-glass opacities consistent with ARDS which worsened over the hospital course. The patients were intubated and brought to the Intensive Care Unit. Whether the patients were placed on ventilators was not specifically stated. All of the patients tested positive for SARS-CoV-2 by 2019 novel coronavirus real time RT-PCR. Notable laboratory findings were the development of elevated ferritin, fibrinogen, prothrombin time, and within 24 hours of death, an increased neutrophil count with relative lymphopenia. D-dimers drawn near the time of death were markedly elevated (1200–2900 ng/mL)."

"All of the lungs were heavy (680–1030 g for left lungs and 800–1050 g for right lungs). The pulmonary arteries at the hilum of each of the lungs were free of thromboemboli. The parenchyma of each of the lungs was diffusely edematous and firm, consistent with the clinical diagnosis of ARDS. Notably, regions of multifocal dark-colored hemorrhage were prominent. In some cases, small, firm thrombi were present in sections of the peripheral parenchyma on gross examination. Major histological findings were bilateral DAD with multifocal hyaline membranes; a comparatively mild-to-moderate lymphocytic infiltrate, composed of a mixture of CD4+ and CD8+ lymphocytes; and desquamated type 2-pneumocytes with apparent viral cytopathic effect consisting of cytomegaly, and enlarged nuclei with bright, eosinophilic nucleoli. The alveolar capillaries were notably thickened, with surrounding edema, and fibrin thrombi were present within capillaries and small vessels. A notable finding was the presence of CD61+ megakaryocytes, possibly representing resident pulmonary megakaryocytes, with significant nuclear hyperchromasia and atypia. These cells were found within alveolar capillaries, often in association with, and actively producing platelets. The fibrin and platelets present within small vessels also appeared to aggregate inflammatory cells, with entrapment of numerous neutrophils." With the exception of the patient on immunosuppression, no significant neutrophilic infiltrate was found within alveoli or the interstitium to suggest secondary infection.

"Examination of the heart was performed in 3 cases, with the hearts ranging in size from 430 to 550 gs (normal: 365 grams±71). The most significant findings were cardiomegaly, and right ventricular dilatation. No case had significant coronary artery stenosis or thrombosis. Histologically, the sections of myocardium did not show any large or confluent areas of myocyte necrosis. However, there was scattered individual cell myocyte necrosis in each heart examined. Rare interstitial small collections of lymphocytes were seen. There was no significant brisk lymphocytic inflammatory infiltrate consistent with the typical pattern of viral myocarditis."

"The relative distribution of dsDNA and RNA in tissue sections was examined with DRAQ5 and SYTO RNA Select fluorescent staining [16]. Virally-infected cells in alveolar spaces showed multinucleation and grouping as evidenced by DNA stain, and abundant RNA present within the cytoplasm. Also noted was entrapment of immune cells, including degenerated neutrophils, within fibrin, and strands of extracellular material with weak DNA staining."

Histological and ultrastructural findings have been reported from autopsies on 12 fatal COVID-19 cases from the University of Washington in conjunction with the Kings County and Snohomish Medical Examiner Offices [17]. "All 12 patients were older with significant preexisting comorbidities. The major pulmonary finding was DAD in the acute and/or organizing phases with virus identified in type I and II pneumocytes by electron microscopy. The kidney demonstrated viral particles in the tubular epithelium, endothelium, and podocytes without significant inflammation. Viral

particles were also observed in the trachea and large intestines. SARS-CoV-2 RNA was detected in the cardiac tissue of a patient with lymphocytic myocarditis. RT-PCR also detected viral RNA in the subcarinal lymph nodes, liver, spleen, and large intestines."

Two cases have been reported from the Icahn School of Medicine at Mount Sinai, New York, New York [18]. "The first patient, a middle-aged male with well-controlled hypertension, was admitted after 9 days with typical COVID-19 symptoms. A nasopharyngeal swab was positive for SARS-CoV-2 by real-time RT-PCR amplification for both the SARS-CoV-2 ORF1 a/b and pan-Sarbecovirus E-gene, but the chest radiograph showed only mild bilateral pulmonary vascular congestion. He was treated for bacterial superinfection, with some improvement, but continued to require supplemental nasal oxygen. Serum ferritin and C-reactive protein were elevated. Repeat chest radiograph on hospital day 8 revealed new dense patchy left mid-lung and retrocardiac opacities, and a hazy opacity in the right lower lung. On day 9, the patient complained of increasing left inspiratory chest pain and tenderness, and 30 minutes later developed pulseless electrical activity."

"The second patient, a middle-aged male with asthma, hypertension and human immunodeficiency virus (HIV) infection controlled on highly-active antiretroviral therapy, was admitted with a 2-day respiratory illness history. A nasopharyngeal swab was positive for SARS-CoV-2. He was febrile on admission, and chest radiography showed multiple bilateral lung opacities. Elevated ferritin and C-reactive protein were noted. His-condition deteriorated, requiring intubation and mechanical ventilator support. Eight days following admission he developed pulseless electrical activity."

"At autopsy, a common notable finding was pulmonary thromboembolism, with occlusion of the right main pulmonary artery in 1 case, and occlusion of both left and right pulmonary arteries in the second. Deep venous thrombosis was found in both cases. Other findings were multiple foci of pulmonary consolidation, cardiomegaly and left ventricular hypertrophy consistent with hypertensive cardiovascular disease. There was no mention of cardiomyocyte injury or myocarditis."

"Ultrastructural examination demonstrated pleomorphic viral-like particles ranging from 60 to 120 nm in distended cytoplasmic vacuoles within the pneumocytes in lung specimens from both cases. The individual spherical viral-like particles displayed distinctive projections with mature particles exhibiting electron dense centers, consistent with the appearance of coronavirus. Fibrin deposition within and outside capillaries as well as pure platelet thrombi also were noted."

4. Houston cases

Case one was a moderately obese (body mass index, BMI 33,8Kg/m²) 62-year-old Hispanic man with a few-day history of respiratory illness who was found dead in his car. A medicolegal autopsy was performed. Nasopharyngeal swab at the time of autopsy tested positive by real time-polymerase chain reaction (RT-PCR) for SARS-CoV-2 virus. Hepatitis panel (A, B, C) was negative. The hemoglobin A1C was 7.0%. The lungs were heavy (right 820 g, left 770 g), but were free of major thromboemboli and hemorrhages. Histologically, the picture was that of early DAD with multiple hyaline membranes accompanied by a focal and mild inflammation with modest numbers of CD3+ lymphocytes and more numerous CD68+ macrophages in some alveolar spaces (Figs. 1 and 2). There also were collections of reactive pneumocytes exhibiting cytomegaly, nucleomegaly with prominent nucleoli, and mitotic figures. Some alveoli showed squamous metaplasia of the alveolar lining, presumably derived from the same reactive pneumocytes. By immunohistochemistry, the pneumocytes in the alveoli were TTF-1 and CK-7 positive and the clusters showing squa-
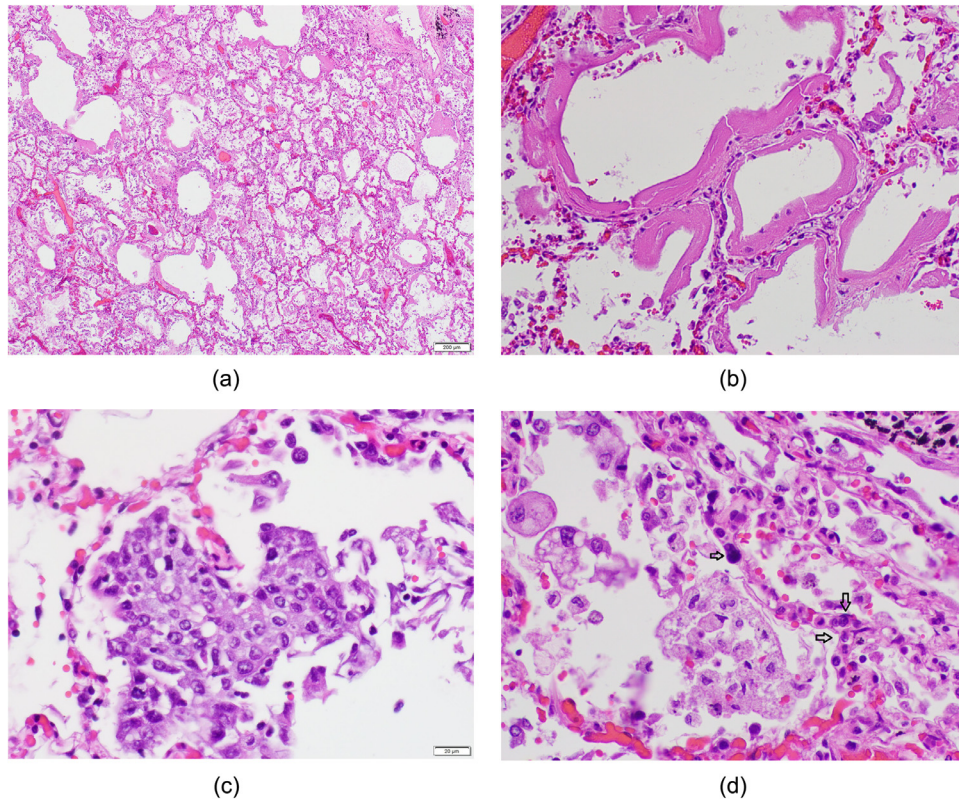
Fig. 1. Houston Case One (HC1). (A) Pulmonary alveoli exhibit congested capillaries, hyaline membranes and increased numbers of mononuclear cells in the alveolar spaces. (B) Hyaline membranes resulting from capillary leak leading to fibrinous exudate and fibrin precipitate. (C) Collection of pneumocytes showing squamous metaplasia. (D) Alveoli exhibiting congested alveolar capillaries containing leukocytes (2 arrows) and a megakaryocyte with large hyperchromatic nucleus (single arrow) and alveolar spaces containing foamy macrophages of variable size. (A, B, C, D; Hematoxylin and eosin stains). (Magnification bar: A 200 µm; B, C, and D 20 µm).
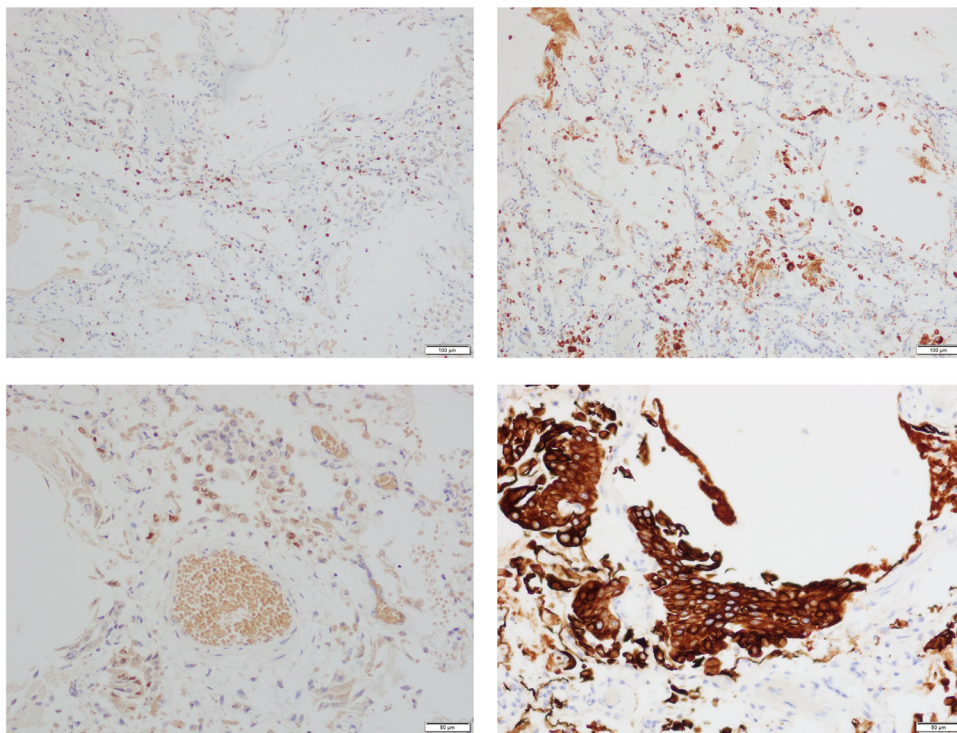

Fig. 2. Houston Case One (HC1). Immunohistochemical findings for lung pathology. Alveoli contain a mildly increased number of CD3+ *T* lymphocytes (A), a moderately increased number of CD68+ macrophages (B) and increased numbers of TTF+ pneumocytes (C). Clusters of pneumocytes exhibit squamous metaplasia as indicated by positive CK 5/6 expression (D). (Magnification bar: A, B, C and D; 100 µm).
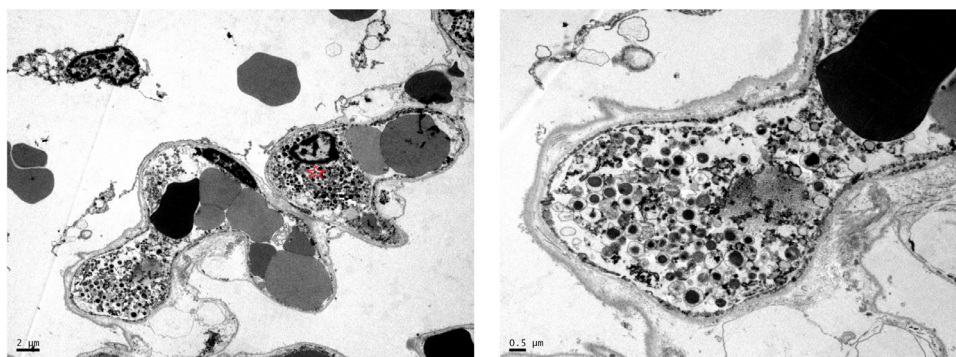
Fig. 3. Houston Case One (HC1). Electron micrographs. (A) Alveolar capillaries contain erythrocytes and neutrophils identified by the presence of characteristic granules (red star). (B) Higher magnification view of cellular 500 nanometer particles which likely represent swollen lysosomes (azurophil granules).
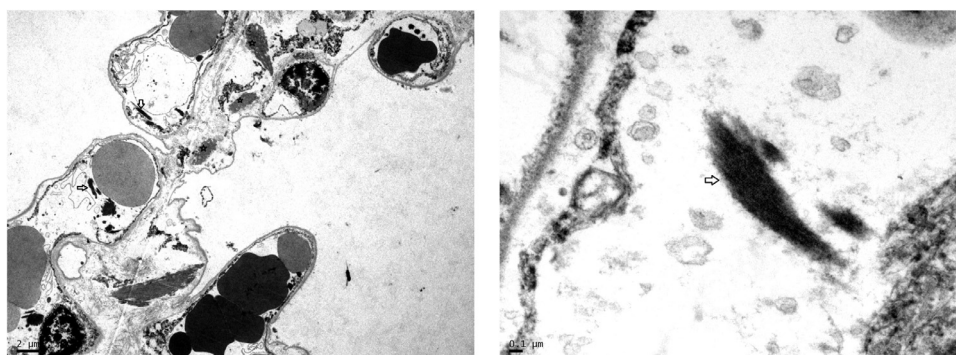

Fig. 4. Houston Case One (HC1). Electron micrographs. (A) Alveolar capillaries contain erythrocytes and strands of electron dense fibrin (arrows). The edematous alveolar septum also has larger precipitates of fibrin outside of the capillary (stars). The alveolar lining cells have been lost. (B) Higher magnification view of fibrin deposit within an alveolar capillary (star).
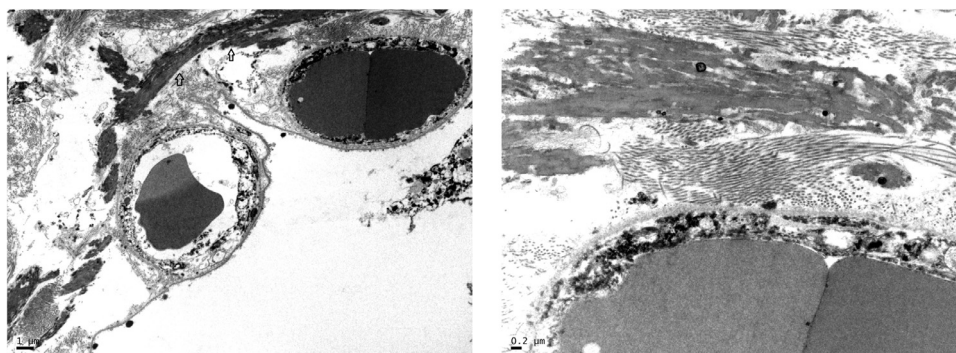

Fig. 5. Houston Case One (HC1). Electron micrographs. (A) Large electron-dense, intra-alveolar fibrin deposits are in close apposition to the alveolar septum (arrow). (B) Higher magnification view of intra-alveolar fibrin deposit intermixed with collagen fibrils.

mous metaplasia were P40 and CK5/6 positive. Many alveolar capillaries contained megakaryocytes identified by large, hyperchromatic nuclei. These cells were CD61+, and numerous small CD61+ particles representing platelets also were present in the capillaries. No microthrombi were identified on histological examination in small pulmonary arteries.

Although no microthrombi were identified on light microscopic examination, electron microscopy revealed strands of precipitated fibrin and entrapped neutrophils within alveolar capillaries as well as larger deposits of fibrin in alveolar spaces (Figs. 3–5). No viral particles were identified in lungs or heart although cytological preservation was suboptimal.

The heart weighed 420 g and had patent coronary arteries with minimal atherosclerosis. The thickness of the left ventricular wall was 1.1 cm and that of the right ventricular wall was 0.2–0.3 cm. The myocardium showed cardiomyocytes with moderately enlarged hyperchromatic nuclei and individual cardiomyocytes with vacuolar degenerative change (Fig. 6). There was no evidence of inflammatory infiltrate indicative of myocarditis. By immunohistochemistry, there were 7–10 or less CD3+ *T* cells and rare CD68+ macrophages per high power field in the myocardium. Lymphocytic infiltrates composed of CD 3+*T* cells with were present in the epicardium with a CD4/CD8 ratio of 2:1. (Fig. 6). Random sections of the sinoatrial and atrioventricular conduction system showed no abnormalities. The liver showed moderate macrovesicular steatosis without evidence of hepatitis (Fig. 6). The kidneys showed evidence of hyaline arteriolosclerosis with glomerulosclerosis. Viral particles were identified in some glomerular endothelial cells. The spleen was enlarged. There was expansion of the red pulp by congestion but also by a lymphoplasmacytic infiltrate (Fig. 7). The white pulp was diminished and shrunken with absence of marginal zones. There were scattered immunoblasts near the edge
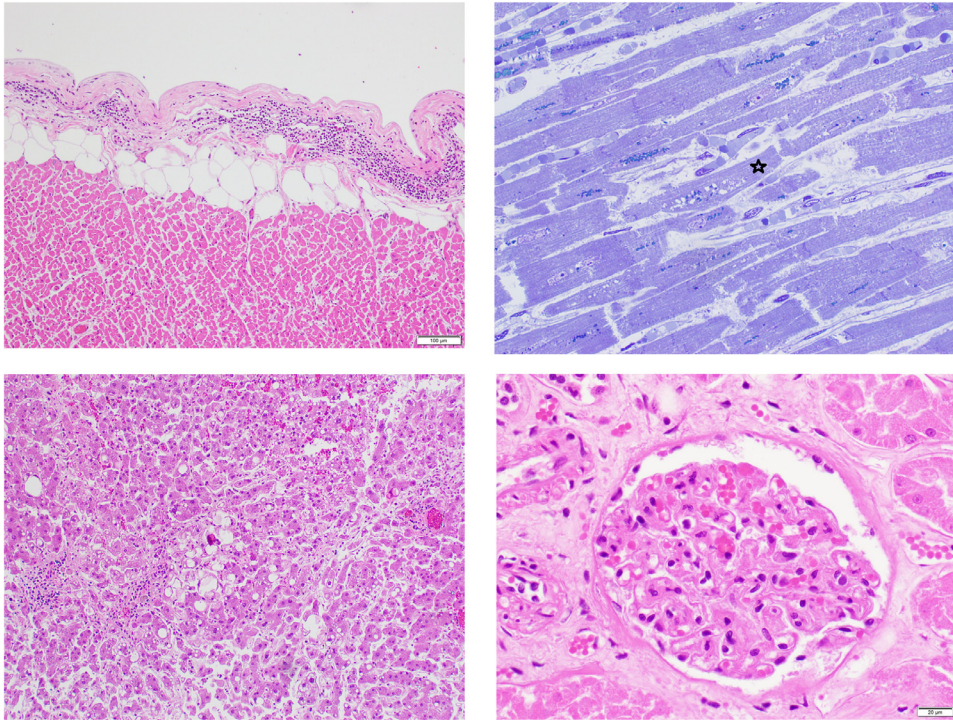
Fig. 6. Houston Case One (HC1). (A) Epicardium exhibits a focus with lymphocytic infiltrate indicative of lymphocytic pericarditis. (B) Myocardium is edematous as manifest as separation of the cardiomyocytes (CMC) and capillaries. The CMC in the center shows vacuolar degenerative change (star). No inflammatory cells are present. (C) Liver shows moderate macro-steatosis and altered, shrunken hepatocytes likely representing incipient apoptosis. (D) Renal glomerulus with focally congested capillaries. (A, C and D, Hematoxylin and eosin stains; B, 1-micron section, toluidine blue stain). (Magnification bar: A and C, 100 μm; B and D, 20 μm).

of the small white pulp and scattered into the red pulp. There were no microthrombi or morphological features of vasculitis or a microangiopathic process. There were no macrophages with features of hemophagocytosis, thus no evidence for hemophagocytic lymphohistiocytosis. The brain was not examined.

Case Two was a 34-year-old obese (BMI 51.65 Kg/m^2) African-American man with a past medical history of hypertension, heart failure with reduced left ventricular ejection fraction (<20%), type II diabetes mellitus and microcytic anemia who presented to the emergency room after developing headache, shortness of breath, cough productive of bloody sputum for 4 days, and fever for 1 day. On admission, chest radiograph showed cardiomegaly and diffuse bilateral interstitial opacities in the lungs. The CT chest findings included diffuse ground glass opacities of rounded morphology involving the upper and lower lobes of both lungs (Fig. 8). The pulmonary artery was dilated at 3.4 cm (normal less than 3.15 cm) indicative of pulmonary hypertension. A pulmonary embolism was not identified. There was global cardiomegaly and a trace pericardial effusion. Electrocardiogram showed left ventricular hypertrophy with left axis deviation. The patient's laboratory findings included white blood cell count of 4.0/μL with 81.5% neutrophils (absolute 3.28), lymphocytes 12.4% (absolute 0.50), monocytes 5.2% (absolute 0.50) eosinophils 0.2%, and basophils 0.5%, platelets 190/μL, hemoglobin (Hg) 11.2 g%, mean corpuscular volume 70.8, and red cell distribution 36. and mildly elevated serum troponin with a peak of 0.22 ng/mL (normal < 0.045 ng/mL). Hemoglobin A1c was 6.3%. On admission brain naturetic peptide was 428 pg/mL and troponin was 0.09 ng/mL (normal <0.045 ng/mL). Troponin later peaked at 0.22 ng/mL. Ferritin, D-dimer, prothrombin time, and partial thomboplastin time were not measured. Creatinine on admission was 1.0 mg/dL (normal 0.7–1.3 mg/dL) and remained normal until a final reading of 2.4 mg/dL.

The patient was initially treated with antibiotics which was deescalated to supportive case when the nasopharyngeal swab

test (RT-PCR) came back positive for SARS-CoV-2 virus. Tests for influenza and respiratory syncytial virus were negative. Working diagnoses in addition to COVID-19 infection were non-ischemic cardiomyopathy (NYHA class 3) with acute on chronic combined systolic and diastolic heart failure. The patient had a 10-day hospital course marked by recurrent fever, episodes of hemoptysis and shortness of breath. He received supplemental oxygen at 3–5 liters per minute but he was never placed on a mechanical ventilator. On the day of his death, he experienced severe worsening of respiratory failure followed by pulseless electrical activity.

At autopsy, the major gross findings were extremely congested lungs (1980 g combined weight) with multiple bilateral segmental pulmonary thromboemboli and multiple areas of hemorrhage, confirmed histologically as acute, unorganized thrombi (Fig. 9). The heart that weighed 1070 g with four-chamber hypertrophy and dilatation and patent coronary arteries with minimal atherosclerosis. The thickness of the left ventricular wall was 1.5–1.6 cm and that of the right ventricular wall was 0.5 cm. The brain was not examined. Histologically the myocardium showed epicardial lymphocytic infiltrates; cardiomyocyte hypertrophy; multifocal interstitial and replacement fibrosis; scattered damaged individual cardiomyocytes, and no inflammatory foci indicative of myocarditis (Fig. 10). By immunohistochemistry, there were 7–10 or less CD3+ T cells and rare CD68+ macrophages per high power field in the myocardium. Lymphocytic infiltrates composed of CD 3+T cells with were present in the epicardium with a CD4/CD8 ratio of 2:1. Random sections of the sinoatrial and atrioventricular conduction system showed no abnormalities. The lungs showed multiple bilateral segmental acute thromboemboli with associated areas of pulmonary hemorrhage and infarction (Fig. 9). Away from these areas, the lungs showed evidence of an interstitial lymphocytic pneumonitis with lymphocytic infiltrates around small blood vessels and in the walls of terminal bronchioles extending into alveolar septae (Fig. 9). Microthrombi were found in some
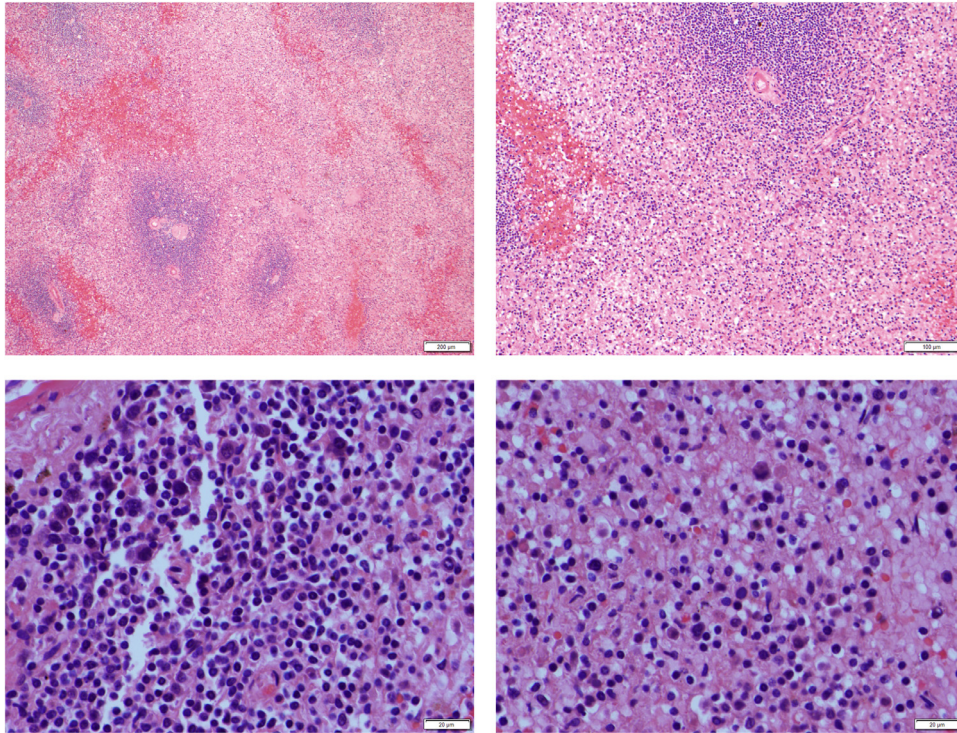
Fig. 7. Houston Case One (HC1). Spleen. (A) Expansion of red pulp and shrinking of white pulp with absent marginal zones. (B) Red pulp with lymphoplasmacytic infiltrate. (C) White pulp with scattered immunoblasts. (D) Red pulp with lymphoplasmacytic infiltrate. (Hematoxylin and eosin stains).
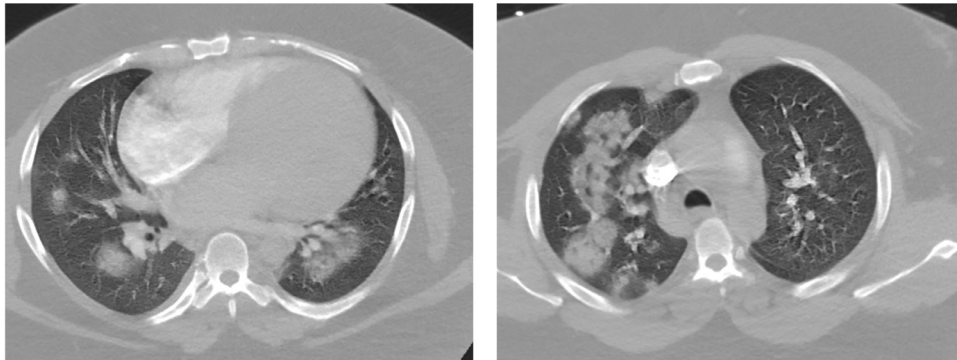

Fig. 8. Houston Case Two (HC2). (A and B) Axial CT images which demonstrate bilateral upper and lower lobe ground-glass and early consolidative alveolar opacities some of rounded morphology, classically described with COVID-19.
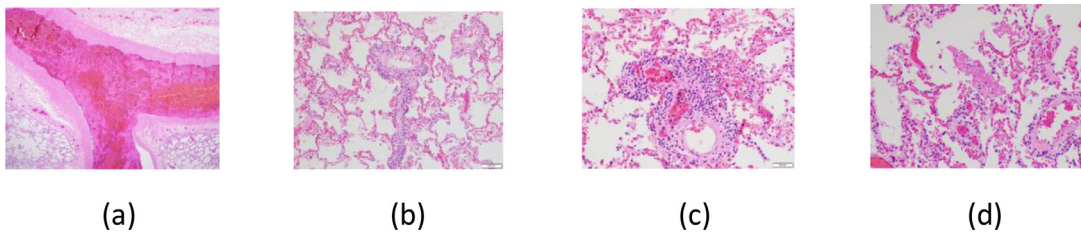

(a)　　　　(b)　　　　(c)　　　　(d)

Fig. 9. Houston Case Two (HC2). (A) Pulmonary thromboembolus obstructing segmental pulmonary artery; one of several in both lungs. (B) Terminal bronchiole with interstitial lymphocytic infiltrates. (C) Interstitial and intra-alveolar infiltrates composed predominantly of lymphocytes. (D) Intra-alveolar fibrin deposit (star). The pulmonary arteriole has a thickened wall indicative of chronic pulmonary hypertension. (A, B, C, D; Hematoxylin and eosin stains). (Magnification bar: A, 500 μm; B, 100 μm; C and D, 50 μm).

pulmonary arterioles. The alveoli contained multiple deposits of fibrin without well-formed hyaline membranes and clusters of pneumocytes. By immunohistochemistry, the pneumocytes in the alveoli were TTF-1 and CK-7 positive and the clusters showing squamous metaplasia were P40 and CK5/6 positive. No microthrombi were identified. The heart showed evidence of individual damaged cardiomyocytes. No inflammatory infiltrates were present. The liver showed moderate macrosteatosis without inflammatory infiltrates. The spleen showed features similar to the spleen of Case 1 with generalized reduction in amount of white pulp and no evidence of hemophagocytic lymphohistiocytosis . The kidneys showed an occasional fibrin-platelet thrombus
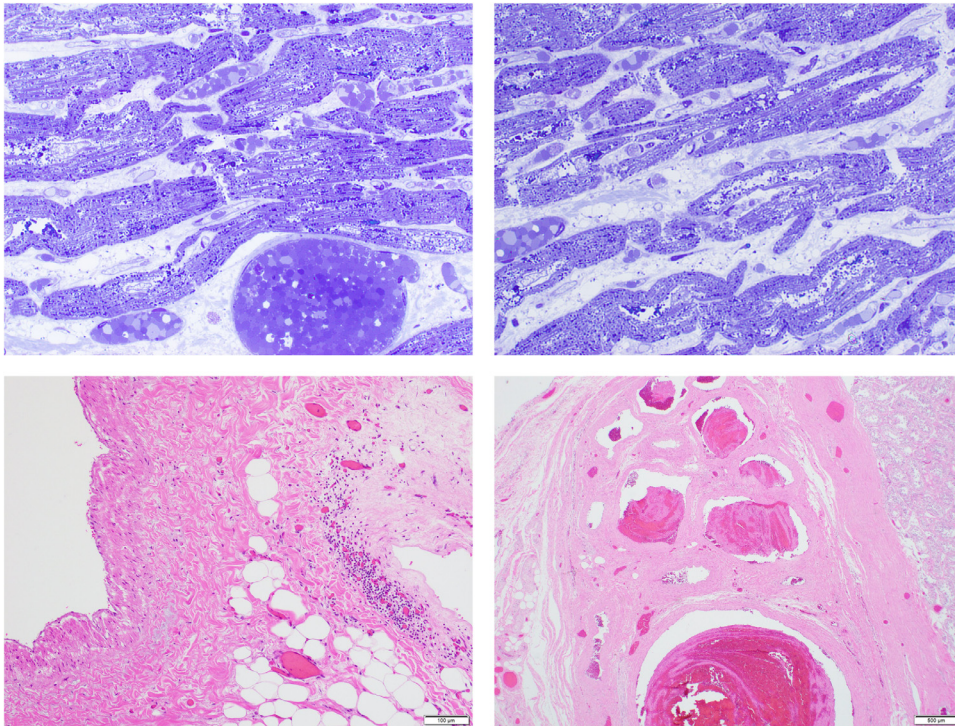
Fig. 10. Houston Case Two (HC2). (A and B) Myocardium is edematous and small blood vessels are congested. The CMC exhibit multifocal vacuolar degenerative changes. No inflammatory cellular infiltrates are present. Note the increased width of these CMC compared to those of HCO (Fig. 6B). The patient's heart weighed 1070 g. (C) The epicardium exhibits a lymphocytic infiltrate adjacent to a vein. (D) Testis with thrombi in peritesticular veins. (A and B, one-micron sections, toluidine blue stain; C and D, hematoxylin and eosin stains). (Magnification bar: A and B, 20 μm; C, 100 μm; D 500 μm).

in renal glomerular capillaries. The testis exhibited thrombi in peritesticular veins (Fig. 10). The brain was not examined.

Case Three was a 48-year-old obese (BMI 35.2 Kg/m^2) Hispanic man who was found dead at his residence. A medicolegal autopsy was performed. Nasopharyngeal swab at the time of autopsy tested positive by RT-PCR for SARS-CoV-2 virus. Screen for influenza viruses was negative. On opening the body, purulent tan opaque watery fluid measuring 500 mL was found in the right pleural cavity. Yellow translucent deposits were focally present of the visceral pleura along the upper/middle interlobar fissure. Organized tan to greenish exudate with fibrotic thickening was present along the parietal and visceral pleural surfaces of the lower lobe. These were features of an empyema. The right lung was collapsed. Minimal fluid was found in the left pleural cavity, pericardial sac and peritoneal cavity. Bacterial cultures of the right pleural cavity and lung grew mixed flora consistent with postmortem contamination. The right and left lungs weighed 1020 and 960 g, respectively. The treacheobronchial tree was lined by a hyperemic red-brown mucosa with no mucous plugs. The major pulmonary arteries were free of thromboemboli. The parenchyma of the lungs was dull red-brown and firm. The heart weighed 670 g. The coronary arteries showed minimal atherosclerosis and were widely patent. Both ventricles were dilated. The thickness of the left ventricular free wall and interventricular septum was 1.6 cm and that of the right ventricle was 0.3 cm.

On histological examination, the right pleura exhibited a necroinflammatory infiltrate overlying cellular granulation tissue confirming the diagnosis of empyema. The right lung showed evidence of atelectasis as well as evidence of DAD. The DAD was more pronounced in the expanded left lung. The changes consisted of multifocal hyaline membranes, intra-alveolar fibrinous exudate, abundant intra-capillary megakaryocytes, numerous intra-alveolar macrophages, and activated type II pneumocytes, along with some neutrophils and intra-alveolar hemorrhage (Fig. 11).

Multifocal lymphocytic infiltrates were present in the epicardium. CMC showed enlarged hyperchromatic nuclei. Individual CMC showed changes of acute injury. No inflammatory cellular infiltrates were found. Additionally, there were prominent foci of CMC disarray, particularly involving the superior portion of the interventricular septum. Many of the intramural coronary arteries showed intimal and medical thickening with luminal narrowing. The myofiber disarray and intramural coronary vasculopathy are diagnostic features of hypertrophic cardiomyopathy. Random sections of the sinoatrial and atrioventricular conduction system showed no abnormalities.

The liver showed moderate macrovesicular steatosis, lymphoplasmacytic triaditis with portal fibrosis and early portal-portal bridging fibrosis. The kidneys showed mild hyaline arteriolosclerosis and periglomerular hyaline arteriolosclerosis with rare holosclerotic glomeruli. The spleen showed lymphocyte depletion in the white pulp with absence of marginal zones; the red pulp was expanded with congestion and hemorrhage; abundant plasma cells were present in the red pulp. The brain showed no significant histopathological change.

5. Discussion

5.1. General

COVID-19 is a viral disease that involves multiple organ systems while usually presenting as an acute febrile respiratory illness [1–6],[19–31]. Acute COVID-19 has 3 distinct phases: early infection, pulmonary and severe hyperinflammation [31]. Prognostic indicators of a more serious and potentially fatal course include older age, lymphopenia, elevated D-dimer level, elevated troponin levels and pre-existing cardiovascular disease, hypertension and diabetes mellitus [19–31]. The pulmonary and cardiovascular systems are majorly affected [29–31].
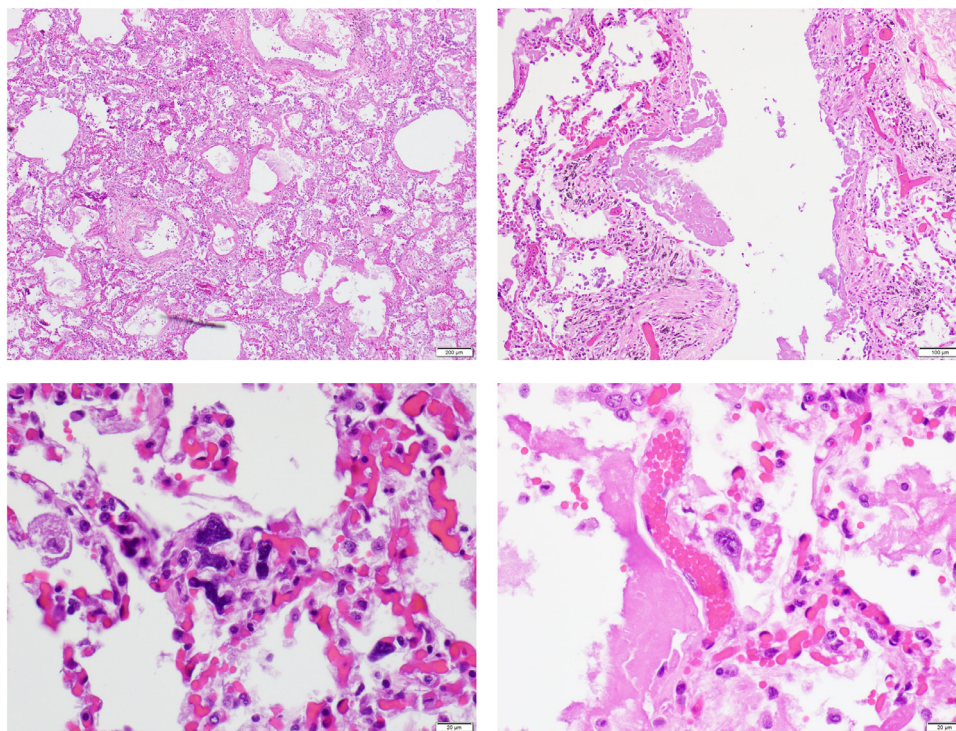
Fig. 11. Houston Case Three (HC3). (A) Pulmonary parenchyma showing interstitial pneumonia with DAD pattern. (B) Bronchiole with fibrinous exudate. (C) Alveolar capillaries contain numerous megakaryocytes with large hyperchromatic nuclei. (D) Alveoli contain enlarged reactive pneumocytes and fibrin deposit. (A, B, C, and D; Hematoxylin and eosin stains). (Magnification bar: A, 200 µm; B, 100 µm; C and D, 20 µm).

In spite of obstacles, autopsies are being performed on COVID-19 patients. We have summarized the first reports of small autopsy series, and added 3 cases from our experience in Houston. The findings are summarized in Tables 1 and 2. From these initially reported cases, a spectrum of pathology of COVID-19 disease is emerging. The picture will be enhanced as more cases are studied and reported.

Based on clinicopathological correlation from these first 23 autopsy cases, the following observations are made: (1) acute COVID-19 pneumonia, not complicated by prolonged hospitalization and ventilator therapy, is a viral interstitial pneumonia characterized by the early exudative phase of DAD with endothelial and epithelial injury, hyaline membranes, reactive pneumocytes with viral cytopathic effect, and mild combined lymphocytic and histiocytic intra-alveolar inflammation [32–34]; 2) a different pulmonary pathology pattern that can be associated wtih an illness of several days is that of a lymphocytic interstitial pneumonitis with intra-alveolar fibrin deposits, which may represent an early stage of acute fibrinous and organizing pneumonia (AFOP) [32,35,36]; (3) the picture of early COVID-19 pulmonary disease is remarkably similar to the DAD described with SARS-CoV virus infection in which both acute interstitial pneumonitis with a DAD pattern and AFOP have been described [37,38]; (4) although not universally found, pulmonary microthrombi are common, consistent with the frequent development of a SARS-CoV-2- induced hypercoagulable state [16]; (5) major pulmonary thromboembolism is a common fatal complication [18]; (6) cardiovascular disease is a frequent co-morbidity in fatal cases [18]; (7) individual cardiomyocyte damage is frequent, probably as a result of infection of endothelial cells, perivascular cells and/or cardiomyocytes (see below); (8) myocarditis is much less common than suggested by elevated serum troponin levels, particularly if high sensitivity troponin is used [39–43]; (9) depletion of white pulp of the spleen occurs as a correlate of the lymphopenia; (10) frequency and severity of target organ involvement in this systemic disease is linked to the distribution of the ACE-2 receptor for the virus [3,4,29–31]; (11) the frequent co-infection with influenza and other viruses makes for difficulties in determining the direct effects of the SARS-CoV-2 virus [44]; (12) antibody-dependent enhancement may be important in determining the variable response to SARS-CoV-2 viral infection [45,46]; (13) treatment strategies should be guided by insights into the pathogenesis and pathophysiology of the disease provided by autopsy studies.

5.2. Pulmonary system

High confidence imaging findings on CT in patients with COVID-19 in the early phase include peripheral and bilateral ground glass opacities sometimes demonstrating a rounded morphology [47–49]. This pattern of imaging is classically seen with evolving pneumonia explaining the causative pattern of lung injury. With disease progression, more areas of consolidation are seen that can progress to diffuse multifocal airspace disease as seen with DAD and ARDS [46–50]. Imaging patterns that suggest an alternative diagnosis include a lobar pattern of consolidation, discrete pulmonary micronodules, pleural effusions and lymphadenopathy. Although the bilateral peripheral distribution of opacities is considered to be characteristic of COVID-19, other viral pneumonias, including those produced by certain strains of influenza, also can have a bilateral distribution of radiographic findings [51,52].

From the analysis of autopsy findings in fatal COVID-19 cases, the pathological correlate of the imaging findings seen early in the course of COVID-19 is the distinctive interstitial pneumonia with DAD pattern. This COVID-19 interstitial pneumonitis can be accompanied by small vessel thrombi with associated hemorrhage in the lung periphery [16]. The COVID-19 interstitial pneumonitis also may be complicated and masked by multiple pulmonary thomboemboli (Houston Case Two and the 2 Mt. Sinai cases).

The pathogenesis of COVID-19 pulmonary disease involves binding of SARS-CoV-2 virus to ACE-2 receptors to pneumocytes and endothelial cells leading to development of acute lung injury

Table 1
Important findings in 23 autopsies subjects with COVID-19

Gender	Male	12
	Female	7
	Not specified	4
Ethnicity	African-American	5
	Hispanic	2
	Not specified	16
Age group	Known: 34–76	21
	Not Specified	2
Comorbidities[*]	Hypertension	10
	Obesity	9
	Type II diabetes mellitus	5
Pulmonary pathology	23	
	Acute pneumonitis	20
	• Interstitial pneumonitis with DAD	16
	• Interstitial lymphocytic pneumonitis	1
	• Insipient interstitial pneumonitis	2
	• Bronchopneumonia with aspiration	1
	Fibrin-rich thrombi in capillaries and small blood vessels	6[§]
	Large pulmonary thromboemboli	5
Cardiac Pathology[†]	23	
	Cardiomegaly, ranging 420–1070 g	13
	Individual cardiomyocyte injury	8
	Lymphocytic epicarditis/pericarditis	3
	Lymphocytic myocarditis	1
Splenic Pathology[†,‡]	6	
	Diminished white pulp with loss of marginal zones	6
	Expansion of red pulp with lymphoplasmacytic infiltrate	3

[*] Does not include WA cases (no specific data on number of cases/comorbidity provided).
[†] No information about cardiac or splenic histology included in report from NY (report does note cardiomegaly in both cases).
[‡] No information about splenic findings included in report from LA.
[§] Includes Tx case #2 but does not include TX case #1 with intravascular fibrin aggregates seen only by EM.

Table 2
Pathophysiological factors in COVID-19 disease

Systems or organs	Pathophysiological factors
Pulmonary	• Viral uptake into vascular endothelium and pneumocytes • Distinctive interstitial pneumonia with intra- and extravascular fibrin deposition, activation of megakaryocytes, intravascular trapping of neutrophils, proliferation of type II pneumocytes, intra-alveolar accumulation of lymphocytes and macrophages • Diffuse alveolar damage with overlapping phases, including hyaline membrane formation, alveolar fibrin deposits, hyper reactive type II pneumocytes with viral cytopathic effects, squamous metaplasia with syncytium, and later organizing phase • Thrombotic microangiopathy • Pulmonary thromboembolism
Cardiovascular system	• Viral uptake into interstitial, perivascular and endothelial cells • Endotheliitis • Microvascular dysfunction • Direct or indirect damage to cardiomyocytes • Myocarditis in some cases • Pericarditis in some cases
Hematologic system	• Virus induced procoagulant stage and coagulopathy • Virus invasion and damage of T lymphocytes resulting in lymphopenia • Depletion of white pulp of the spleen • Predisposition to deep vein thrombosis and pulmonary thromboembolism

manifest as DAD [3,4,29]. The inflammatory reaction in DAD involves endothelial cell damage, capillary leak, activation of type II pneumocytes, and involvement of polarized pulmonary macrophages [32–34],[53–57]. There is also evidence for a role for pulmonary thrombotic microangiopathy in COVID-19 pulmonary disease [16]. The pathophysiology of disease progression likely involves hypoxic pulmonary vasoconstriction [58].

Also, the possible relationships and merging of the patterns of DAD and organizing pneumonia, also known as bronchiolitis obliterans combined organizing pneumonia and cryptogenic organizing pneumonia, as well as a variant know as AFOP, need further study [32–36],[59]. The dominant feature of AFOP is intra-alveolar fibrin "balls" or aggregates, typically in a patchy distribution. Organizing pneumonia in the form of luminal loose fibroblastic tissue is present surrounding the fibrin [32–34]. Hyaline membranes are absent. The acute interstitial pneumonia of Hamman-Rich syndrome is characterized by the simultaneous presence of both acute and organizing DAD [32,59].

Copin et al. recently have reported the findings from postmortem biopsies in 6 patients [36]. The 1 patient who died after a 5-day course showed a lymphocytic viral pneumonia with DAD pattern. The 5 other patients who died after about 20 days of symptoms had the histological pattern of AFOP. Correlation with pathophysiological showed that the first patient had a type L pat-

tern of low pulmonary elastance whereas the other 5 patients had a type H pattern of high pulmonary elastance. Our patient who died after a 10–14-day course had a lymphocytic interstitial pneumonitis with intra-alveolar fibrin deposits and no hyaline membranes or foci of organizing pneumonia. This pattern may represent a transition from the DAD to the AFOP patterns. Interstitial pneumonitis with DAD and AFOP patterns has been described in the original SARS disease. Going forward, more extensive and detailed correlation of the clinical, imaging and pathological changes of the pulmonary component of COVID-19 is needed.

5.3. Cardiovascular system

The cardiovascular system is majorly impacted in many patients with COVID-19 disease. Clinical features are indicative of acute myocardial injury as manifested by elevated serum troponin level, arrhythmias and ST segment elevation and/or depression on electrocardiogram in the absence of obstructive coronary artery disease [29–31],[60–64].

Tavazzi et al. obtained an endomyocardial biopsy from a 69-year-old patent with a flu-like illness due to SARS-CoV-2 infection that was successfully treated with venous-arterial extracorporeal membrane oxygenation and mechanical ventilation. Endomyocardial biopsy demonstrated low-grade myocardial inflammation and viral particles in the myocardial interstitial cells but not in cardiomyocytes or endothelial cells [65]. The ultrastructural study demonstrated single or small groups of viral particles with the morphology (dense round viral envelope and electron-dense spike-like structures on their surface) and size (variable between 70 and 120 nm) of coronaviruses [66]. The authors interpreted the findings as evidence of direct involvement of the myocardium during a viremic phase or migration of infected macrophages from the lung. Grimes et al. demonstrated 60–120 nm "viral-like" particles in distended cytoplasmic vacuoles within pneumocytes as well as rupture of the cytoplasmic vacuoles with release of the virus-like particles into the alveolar lumen [18]. The individual spherical viral-like particles had distinctive projections with mature particles exhibiting electron dense centers, consistent with the appearance of coronaviruses.

Mild to moderate troponin elevations, particularly if measured by the high sensitivity troponin assays (hs-Tn), must be interpreted with caution regarding the magnitude of myocardial injury and may not reflect extensive irreversible myocardial injury due to myocardial ischemia or myocardial inflammation. Overt myocarditis, characterized by inflammatory cellular infiltrates with associated cardiomyocyte damage, does occur with COVID-19 infection but is much less common than suggested by overinterpretation of troponin levels [39–43]. Right heart strain with pulmonary thromboembolism also can be associated with elevated troponin level.

Chen et al. hypothesized that pericytes may be infected by the SARS-CoV-2 virus and cause capillary endothelial cell and microvascular dysfunction that may cause individual cardiomyocte necrosis. This can explain the frequent occurrence of mild to moderate troponin elevations in patients with COVID-19 [67]. Direct involvement of coronary arteries in viral infections has been considered in the pathogenesis of clinical cardiac manifestations of these diseases [68]. However, inflammation of the coronary arteries has not been observed in the Houston COVID-19 autopsy cases. Another manifestation of cardiac involvement in COVID-19 may be stress induced, i.e., Takotsubo cardiomyopathy [69,70].

Pre-existing heart disease, diabetes mellitus and obesity clearly predispose to adverse outcome from COVID-19 infection. Of note, the 3 Houston cases were obese men with evidence of chronic heart disease: hypertension-related left ventricular hypertrophy, dilated cardiomyopathy and hypertrophic cardiomyopathy. The nature of the interactions requires further study. Another phenomenon is that the COVID-19 pandemic is causing patients with acute coronary syndromes to delay obtaining treatment or avoid presenting to the hospital for medical attention, with potentially fatal consequences [62]. Patients with cardiac transplants may be at particularly increased risk [71].

Influenza infection imparts an increased risk for acute myocardial infarction and sudden cardiac death in subsequent months following the acute illness. It is important to determine if COVID-19 infection imparts a similar risk for subsequent cardiovascular events [72,73].

5.4. Systemic manifestations of COVID-19

COVID-19 infection of organs is initiated by binding of the virus to the ACE-2 receptor on a cell [3,4,29–31,67]. Thus, the distribution of the ACE-2 receptor in various cell types in different organs determines the involvement of these sites in the progression of COVID-19. The diseases progresses from a pulmonary infection to a systemic disease. In addition to heart and lung, target organ involvement of brain stem, liver and kidneys have been reported [74–80]. In this report, involvement of the spleen is documented. Even though histological changes in the kidney are relatively mild, many COVID-19 patients are experiencing clinical features of acute renal injury and failure [78–80].

Clinical reports have associated severe pneumonia and fatal outcomes in SARS-CoV-2 with elevated levels of D-dimer and fibrin degradation products, suggesting derangement of coagulation activation and consequently a potential disposition to thromboembolic events. [19–31]. Grimes et al. point out that several viral infections have been associated with coagulation disorders that may lead to thrombosis and disseminated intravascular coagulation (DIC) [18]. Both influenza virus and SARS have been associated with pulmonary intravascular thrombi formation and fibrin deposition likely as a result of DIC and microthrombosis. In SARS coronavirus infection, increased production of a novel pro-coagulant by infected cells due to increased hfg12 gene transcription induced by viral nucleocapsid (N) protein has been proposed as a mechanism contributing to thrombosis [18,81].

Fox et al. noted pulmonary microvascular thrombi, CD4+ *T* cells around the thrombosed vessels, focal hemorrhages, abundant megakaryocytes in pulmonary capillaries, platelet aggregation, platelet-rich clots, associated entrapment of neutrophils, and fibrin deposits inside and outside of capillaries [16]. We also observed entrapment of neutrophils in capillaries and fibrin deposits within and outside of capillaries. We concur with the suggestion of Fox et al. that an important pathogenic mechanism of fatal COVID-19 disease is a thrombotic microangiopathy primarily involving the lungs. Variation in the demonstration of microthombi in the lungs may relate to the stage of the coagulopathy at the time of death. In DIC, microthrombi are found in multiple organs in relationship to the peak of clot formation but may not be found when the DIC has progressed to depletion of clotting factors and activation of fibrinolysis [82–86].

Endothelial cell infection has been noted in at least two studies [17,84]. Virus-induced endotheliitis appears to be an important underlying mechanism causing vascular dysfunction and thrombotic events in lung, kidney, brain, and possibly the heart and other organs (Fig. 12) [67,87]. Also, the influence of co-infection with SARS-CoV-2 and other viruses likely is important in influencing the outcome in individual patients [29,44]. This phenomenon may be involved in the recently reported development of a clinical picture with features of atypical Kawasaki disease in some children with COVID-19 termed pediatric multi-system inflammatory syndrome [88].
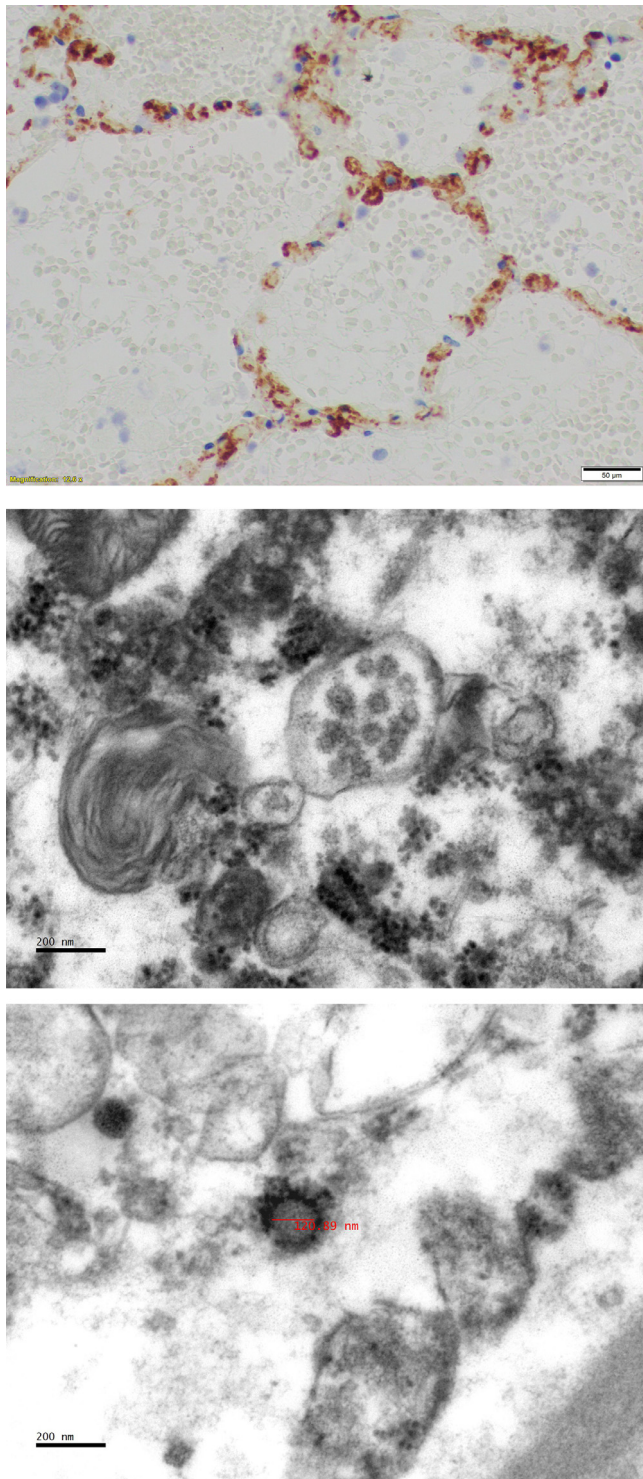
Fig. 12. (A) Immunohistochemistry for CD61 (Glycoprotein IIIa) shows numerous megakaryocytes and platelets (small punctate bodies) in alveolar capillaries. From Houston Case Two (HC2). (Magnification bar, 20 μm). (B) Electron micrograph shows a collection of viral particles in a vacuole inside a renal glomerular endothelial cell from Houston Case One (HC1). X50,000. (C) Electron micrograph of a single 100 nanometer viral particle free in the cytoplasm of a renal glomerular endothelial cell from HC1. Note the nucleocapsid and membrane spike proteins. X50,000.

5.5. Conclusions

Autopsy studies have established that COVID-19 is a systemic disease with major involvement of the cardiovascular and pulmonary systems and with the expected accompaniment of major activation of the inflammatory and immune systems [89,90]. The autopsy studies also provide evidence that SARS-COV-2 patients have a baseline hypercoagulable state and are at increased risk for pulmonary thrombotic microangiopathy as well as the development of deep vein thromboses and major pulmonary thromboembolism. The autopsy findings support evaluation and management for coagulopathy early in the course of disease and judicious use of prophylactic anticoagulants while hospitalized [91–94].

The initial approach to acute therapy for COVID-19 patients with life-threatening respiratory failure has involved administration of supplemental oxygen, artificial ventilation and use of the extracorporeal membrane oxygenator when necessary [95]. Additional approaches and strategies for treatment of COVID-19 patients are actively being pursued, and they are clearly needed [96,97,98]. Autopsies on COVID-19 patients need to continue to be performed to further elucidate the natural history of the disease and to guide the development of optimal therapeutic regimens. A recent report of 21 autopises of COVID-19 patients from Basel, Switzerland provides further confirmation of the findings in the present study [99].

Declaration of Competing Interest

None.

References

[1] Wuhan Municipal Health Commission. [Report of clustering pneumonia of unknown etiology in Wuhan City] (In Chinese). Available at: http://wjw.wuhan.gov.cn/front/web/showDetail/2019123108989; 2019 Accessed April 15, 2020.

[2] World Health Organization (WHO). Pneumonia of unknown cause – China 2020. Available at: https://www.who.int/csr/don/05-january-2020-pneumonia-of-unkown-cause-china/en/; Accessed April 15, 2020.

[3] Zhu N, Zhang D, Wang W, Li X, Yang B, Song J, et al. A novel coronavirus from patients with pneumonia in China, 2019. N Engl J Med 2020;382(8):727–33. doi:10.1056/NEJMoa2001017.

[4] Scherer A. Genetic analysis of the covid-19 virus and other pathogens. Golden Helix; 2020. Available at https://www.goldenhelix.com/resources/ebooks/genetic-analysis-covid-19-other-pathogens.html Accessed April 15, 2020.

[5] Guan WJ, Ni ZY, Hu Y, Liang WH, Ou CQ, He JX, et al. Clinical Characteristics of Coronavirus Disease 2019 in China. N Engl J Med. 2020;382(18):1708–20. doi:10.1056/NEJMoa2002032.

[6] Chen N, Zhou M, Dong X, Qu J, Gong F, Han Y, et al. Epidemiological and clinical characteristics of 99 cases of 2019 novel corona virus pneumonia in Wuhan, China: a descriptive study. Lancet 2020;395(10223):507–13. doi:10.1016/S0140-6736(20)30211-7.

[7] Barth RF, Xu X, Buja LM. A call for action: the need for autopsies to determine the full extent of organ involvement associated with COVID-19 infection. Chest 2020 Apr 10 [Epub ahead of print]. doi:10.1016/j.chest.2020.03.060.

[8] Buja LM, Barth RF, Krueger GR, Brodsky SV, Hunter RL. The importance of the autopsy in Medicine: perspectives of pathology colleagues. Acad Pathol 2019;6:2374289519834041. doi:10.1177/2374289519834041.

[9] Occupational Safety and Health Administration (OSHA) Available at: https://www.osha.gov/Publications/OSHA3990.pdf; 2020 Accessed April 15, 2020.

[10] Centers for Disease Control and Prevention (CDC). Collection and submission of postmortem specimens from deceased persons with known or suspected COVID-19, march 2020 (Interim guidance); 2020. Available at https://www.cdc.gov/coronavirus/2019-ncov/hcp/guidance-postmortem-specimens.html Accessed April 15, 2020.

[11] P.A. Harris, MD, MA, President, American Medical Association. Defending science in a time of fear and uncertainty. Available at:https://www.ama-assn.org/about/leadership/defending-science-time-fear-and-uncertainty?utm_source=BulletinHealtcare&utm_medium=email&utm_term=041120&utm-content=physicians&utm; 2020 Accessed April 15, 2020.

[12] Liu Q, Wang RS, Qu GQ, Wang YY, Liu P, Zhu YZ, et al. Gross examination report of a COVID-19 death autopsy. Fa Yi Xue Za Zhi 2020;36(1):21–3. doi:10.12116/j.issn.1004-5619.2020.01.005.

[13] Xu Z, Shi L, Wang Y, Huang L, Zhang C, Liu S, et al. Pathological findings of COVID-19 associated respiratory distress syndrome. Lancet Respir Med 2020. doi:10.1016/S2213-2600(20)3006-X.

[14] Tian S, Hu W, Niu L, Liu H, Xu H, Xiao SY. Pulmonary pathology of early-phase 2019 novel coronavirus (COVID-19) pneumonia in two patients with lung cancer. J Thorac Oncol 2020 [Epub ahead of print]. doi:10.1016/j.jtho.2020.02.010.

[15] Barton LM, Duval EJ, Stroberg E, Ghosh S, Mukhopadhyay S. COVID-19 autopsies, Oklahoma, USA. Am J Clin Pathol 2020 XX1–9. doi:10.1093/ajcp/aqaa062.

[16] Fox SE, Akmatbekov A, Harbert JL, Li G, Brown JQ, Vander Heide RS. Pulmonary and cardiac pathology in COVID-19: the first autopsy series from New Orleans. MedRxiv 2020. Available at https://doi.org/10.1101/2020.04.06.20050575 Accessed April 15, 2020.

[17] Bradley B.T., Maioli H., Johnson R., Chaudhry I., Fink S.L., Xu H., Najafian B., Marshall D., Lacy J.M., Williams T., Yarid N. Histopathology and ultrastructural findings of fatal COVID-19 infections. MedRxiv. Available at:https://www.medrxiv.org/content/10.1101/2020.04.17.20058545v1. Posted April 21, 2020.

[18] Grimes Z, Bryce C, Sordillo EM, Gordon RE, Reidy J, Paniz Mondolfi A, Fowkes M. Fatal pulmonary thromboembolism in SARS-CoV-2-infection. Cardiovasc Pathol 2020 In press.

[19] Yang X, Yu Y, Xu J, Shu H, Xia J, Liu H, et al. Clinical course and outcomes of critically ill patients with SARS-CoV-2 pneumonia in Wuhan, China: a single-centered, retrospective, observational study [published online ahead of print, 2020 Feb 24] [published correction appears in Lancet Respir Med. 2020 Apr;8(4):e26]. Lancet Respir Med 2020. doi:10.1016/S2213-2600(20)30079-5.

[20] Ruan Q, Yang K, Wang W, Jiang L, Song J. Clinical predictors of mortality due to COVID-19 based on an analysis of data of 150 patients from Wuhan, China [published online ahead of print, 2020 Mar 3] [published correction appears in Intensive Care Med 2020 Apr 6]. Intensive Care Med 2020:1–3. doi:10.1007/s00134-020-05991-x.

[21] Zhou F, Yu T, Du R, Fan G, Liu Y, Liu Z, et al. Clinical course and risk factors for mortality of adult inpatients with COVID-19 in Wuhan, China: a retrospective cohort study [published correction appears in Lancet. 2020 Mar 28;395(10229):1038] [published correction appears in Lancet. 2020 Mar 28;395(10229):1038]. Lancet 2020;395(10229):1054–62. doi:10.1016/S0140-6736(20)30566-3.

[22] Guo W, Li M, Dong Y, Zhou H, Zhang Z, Tian C, et al. Diabetes is a risk factor for the progression and prognosis of COVID-19. Diabetes Metab Res Rev 2020:e3319 [Epub ahead of print]. doi:10.1002/dmrr.3319.

[23] Chen G, Wu D, Guo W, Cao Y, Huang D, Wang H, et al. Clinical and immunological features of severe and moderate coronavirus disease 2019. J Clin Invest. 2020:137244 [Epub ahead of print]. doi:10.1172/JCI137244.

[24] Wu C, Chen X, Cai Y, Xia J, Zhou X, Xu S, et al. Risk Factors associated with acute respiratory distress syndrome and death in patients with coronavirus disease 2019 pneumonia in Wuhan, China. JAMA Intern Med 2020:e200994 [Epub ahead of print]. doi:10.1001/jamainternmed.2020.0994.

[25] Qiu H, Wu J, Hong L, Luo Y, Song Q, Chen D. Clinical and epidemiological features of 36 children with coronavirus disease 2019 (COVID-19) in Zhejiang, China: an observational cohort study. Lancet Infect Dis 2020 S1473-3099(20)30198-5 [Epub ahead of print]. doi:10.1016/S1473-3099(20)30198-5.

[26] Zhang JJ, Dong X, Cao YY, Yuan YD, Yang YB, Yan YQ, et al. Clinical characteristics of 140 patients infected with SARS-CoV-2 in Wuhan, China. Allergy 2020 [Epub ahead of print]. DOI:2020;10.1111/all.14238. doi:10.1111/all.14238.

[27] Richardson S, Hirsch JS, Narasimhan M, Crawford JM, McGinn T, Davidson KW, et al. Presenting characteristics, comorbidities, and outcomes among 5700 patients hospitalized with COVID-19 in the New York City Area [published online ahead of print, 2020 Apr 22]. JAMA 2020 10.1001/jama.2020.6775. doi:10.1001/jama.2020.6775.

[28] Henry BM, de Oliveira MHS, Benoit S, Plebani M, Lippi G. Hematologic, biochemical and immune biomarker abnormalities associated with severe illness and mortality in coronavirus disease 2019 (COVID-19): a meta-analysis [published online ahead of print, 2020 Apr 10]. Clin Chem Lab Med 2020 /j/cclm.ahead-of-print/cclm-2020-0369/cclm-2020-0369.xml. doi:10.1515/cclm-2020-0369.

[29] Geng Y-J, Wei Z-Y, Qian H-Y, Huang J, Lodato R, Castriotta R. Pathopysiological characteristics and therapeutic approaches for pulmonary injury and cardiovascular complications of coronavirus disease 2019. Cardiovasc Pathol 2020 In press.

[30] Madjid M, Safavi-Naeini P, Solomon SD, Vardeny O. Potential effects of coronaviruses on the cardiovascular system: a review. JAMA Cardiol 2020 10.1001/jamacardio.2020.1286. doi:10.1001/jamacardio.2020.1286.

[31] Akhmerov A, Marban E. COVID-19 and the Heart [published online ahead of print, 2020 Apr 7]. Circ Res 2020 10.1161/CIRCRESAHA.120.317055. doi:10.1161/CIRCRESAHA.120.317055.

[32] Cheung OY, Graziano P, Smith ML. Acute lung injury. In: Leslie KO, Wick MR, editors. Practical pulmonary pathology: a diagnostic approach. 2nd edition Philadelphia: Elsevier Saunders; 2018. p. 125–46.

[33] Tomashefski JF Jr. Pulmonary pathology of acute respiratory distress syndrome. Clin Chest Med 2000;21(3):435–66. doi:10.1016/s0272-5231(05)70158-1.

[34] Mandal RV, Mark EJ, Kradin RL. Megakaryocytes and platelet homeostasis in diffuse alveolar damage. Exp Mol Pathol 2007;83(3):327–31. doi:10.1016/j.yexmp.2007.08.005.

[35] Beasley MB, Franks TJ, Galvin JR, Gochuico B, Travis WD. Acute fibrinous and organizing pneumonia: a histological pattern of lung injury and possible variant of diffuse alveolar damage. Arch Pathol Lab Med 2002;126(9):1064–70. doi:10.1043/0003-9985(2002)126(1064:AFAOP)2.0.CO;2.

[36] Copin MC, Parmentier E, Duburcq T, Poissy J, Mathieu DLille COVID-19 ICU and Anatomopathology Group. Time to consider histologic pattern of lung injury to treat critically ill patients with COVID-19 infection [published online ahead of print, 2020 Apr 23]. Intensive Care Med 2020:1–3. doi:10.1007/s00134-020-06057-8.

[37] Hwang DM, Chamberlain DW, Poutanen SM, Low DE, Asa SL, Butany J. Pulmonary pathology of severe acute respiratory syndrome in Toronto. Mod Pathol 2005;18(1):1–10. doi:10.1038/modpathol.3800247.

[38] Gu J, Korteweg C. Pathology and pathogenesis of severe acute respiratory syndrome. Am J Pathol 2007;170(4):1136–47. doi:10.2353/ajpath.2007.061088.

[39] Buja LM, Zehr B, Lelenwa L, Ogechukwu E, Zhao B, Dasgupta A, et al. Clinicopathological complexity in the application of the universal definition of myocardial infarction. Cardiovasc Pathol 2020;44:107153. doi:10.1016/j.carpath.2019.107153.

[40] Buja LM, Ottaviani G, Ilic M, Zhao B, Lelenwa LC, Segura AM, et al. Clinicopathological manifestations of myocarditis in a heart failure population. Cardiovasc Pathol 2020;45:107190. doi:10.1016/j.carpath.2019.107190.

[41] Bularga A, Lee KK, Stewart S, Ferry AM, Chapman AR, Marshall L, et al. High-sensitivity troponin and the application of risk stratification thresholds in patients with suspected acute coronary syndrome. Circulation 2019;140(19):1557–68. doi:10.1161/CIRCULATIONAHA.119.042866.

[42] Lippi G, Lavie CJ, Sanchis-Gomar F. Cardiac troponin I in patients with coronavirus disease 2019 (COVID-19): evidence from a meta-analysis. Prog Cardiovasc Dis 2020 [Epub ahead of print]. doi:10.1016/j.pcad.2020.03.001.

[43] Chapman AR, Bularga A, Mills NL. High-sensitivity cardiac troponin can be an ally in the fight against COVID-19. Circulation 2020 10.1161/CIRCULATIONAHA.120.047008 [Epub ahead of print]. doi:10.1161/CIRCULATIONAHA.120.047008.

[44] Du Y, Tu L, Zhu P, Mu M, Wang R, Yang P, et al. Clinical Features of 85 Fatal Cases of COVID-19 from Wuhan: A Retrospective Observational Study. Am J Respir Crit Care Med 2020 10.1164/rccm.202003-0543OC. doi:10.1164/rccm.202003-0543O.

[45] Tetro JA. Is COVID-19 receiving ADE from other coronaviruses? Microbes Infect 2020;22(2):72–3. doi:10.1016/j.micinf.2020.02.006.

[46] Sharma A. It is too soon to attribute ADE to COVID-19. Microbes Infect 2020 pii: S1286-4579(20)30051-4[Epub ahead of print]. doi: 10.1016/j.micinf.2020.03. doi:10.1016/j.micinf.2020.03.005.

[47] Bai HX, Hsieh B, Xiong Z, Halsey K, Choi JW, Tran TML, Pan I, Shi LB, Wang DC, Mei J, Jiang XL, Zeng QH, Egglin TK, Hu PF, Agarwal S, Xie F, Li S, Healey T, Atalay MK, Liao WH. Performance of radiologists in differentiating COVID-19 from viral pneumonia on chest CT. Radiology 2020;10:200823 [Epub ahead of print]. doi:10.1148/radiol.2020200823.

[48] Chung M, Bernheim A, Mei X, Zhang N, Huang M, Zeng X, Cui J, Xu W, Yang Y, Fayad ZA, Jacobi A, Li K, Li S, Shan H. CT Imaging Features of 2019 Novel Coronavirus (2019-nCoV). Radiology 2020;295(1):202–7. doi:10.1148/radiol.2020200230.

[49] Simpson S, Kay F, Abbara S, Bhalla S, Chung JH, Chung M, et al. Radiological society of north America expert consensus statement on reporting chest CT findings related to COVID-19. Endorsed by the society of thoracic radiology, the American college of radiology, and RSNA. J Thorac Imaging 2020 10.1097/RTI.0000000000000524. doi:10.1097/RTI.0000000000000524.

[50] Torrealba JR, Fisher S, Kanne JP, Butt YM, Glazer C, Kershaw C, et al. Pathology-radiology correlation of common and uncommon computed tomographic patterns of organizing pneumonia. Hum Pathol 2018;71:30–40. doi:10.1016/j.humpath.2017.10.028.

[51] Ruuskanen O, Lahti E, Jennings LC, Murdoch DR. Viral pneumonia. Lancet 2011;377(9773):1264–75. doi:10.1016/S0140-6736(10)61459-6.

[52] Ishiguro T, Takayanagi N, Kanauchi T, Uozumi R, Kawate E, Takaku Y, et al. Clinical and radiographic comparison of influenza virus-associated pneumonia among three viral subtypes. Intern Med 2016;55(7):731–7. doi:10.2169/internalmedicine.55.5227.

[53] Castro CY. ARDS and diffuse alveolar damage: a pathologist's perspective. Semin Thorac Cardiovasc Surg 2006;18(1):13–19. doi:10.1053/j.semtcvs.2006.02.001.

[54] Cardinal-Fernández P, Lorente JA, Ballén-Barragán A, Matute-Bello G. Acute respiratory distress syndrome and diffuse alveolar damage. New insights on a complex relationship. Ann Am Thorac Soc 2017;14(6):844–50. doi:10.1513/AnnalsATS.201609-728PS.

[55] Song C, Li H, Li Y, Dai M, Zhang L, Liu S, et al. NETs promote ALI/ARDS inflammation by regulating alveolar macrophage polarization. Exp Cell Res 2019;382(2):111486. doi:10.1016/j.yexcr.2019.06.031.

[56] Morrell ED, Bhatraju PK, Mikacenic CR, Radella 2nd F, Manicone AM, Stapleton RD, et al. Alveolar macrophage transcriptional programs are associated with outcomes in acute respiratory distress syndrome. Am J Respir Crit Care Med 2019;200(6):732–41. doi:10.1164/rccm.201807-1381OC.

[57] Xiong Y, Liu Y, Cao L, Wang D, Guo M, Jiang A, et al. Transcriptomic characteristics of bronchoalveolar lavage fluid and peripheral blood mononuclear cells in COVID-19 patients. Emerg Microbes Infect 2020;9(1):761–70. doi:10.1080/22221751.2020.1747363.

[58] Lumb AB, Slinger P. Hypoxic pulmonary vasoconstriction: physiology and anesthetic implications. Anesthesiology 2015;122(4):932–46. doi:10.1097/ALN.0000000000000569.

[59] Hashisako M, Fukuoka J, Smith ML. Chronic diffuse lung diseases. In: Leslie KO, Wick MR, editors. Practical pulmonary pathology: a diagnostic approach. 2nd edition Philadelphia: Elsevier Saunders; 2018. p. 227–98.

[60] Bansal M. Cardiovascular disease and COVID-19. Diabetes Metab Syndr 2020;14(3):247–50 [Epub ahead of print]. doi:10.1016/j.dsx.2020.03.013.

[61] Guo T, Fan Y, Chen M, Wu X, Zhang L, He T, et al. Cardiovascular Implications of Fatal Outcomes of Patients With Coronavirus Disease 2019 (COVID-19). JAMA Cardiol 2020:e201017 [Epub ahead of print]. doi:10.1001/jamacardio.2020.1017.

[62] Tam CF, Cheung KS, Lam S, Wong A, Yung A, Sze M, et al. Impact of coronavirus disease 2019 (COVID-19) outbreak on ST-segment-elevation myocardial infarction care in Hong Kong, China. Circ Cardiovasc Qual Outcomes 2020 CIRCOUTCOMES120006631. doi:10.1161/CIRCOUTCOMES.120.006631.

[63] He XW, Lai JS, Cheng J, Wang MW, Liu YJ, Xiao ZC, et al. [Impact of complicated myocardial injury on the clinical outcome of severe or critically ill COVID-19 patients]. Zhonghua Xin Xue Guan Bing Za Zhi 2020;48(0):E011 (In Chinese with English Abstract). doi:10.3760/cma.j.cn112148-20200228-00137.

[64] Inciardi RM, Lupi L, Zaccone G, Italia L, Raffo M, Tomasoni D, et al. Cardiac involvement in a patient with coronavirus disease 2019 (COVID-19). JAMA Cardiol 2020 10.1001/jamacardio.2020.1096 [Epub ahead of print]. doi:10.1001/jamacardio.2020.1096.

[65] Tavazzi G, Pellegrini C, Maurelli M, Belliato M, Sciutti F, Bottazzi A, et al. Myocardial localization of coronavirus in COVID-19 cardiogenic shock. Eur J Heart Fail 2020 10.1002/ejhf.1828 [Epub ahead of print]. doi:10.1002/ejhf.1828.

[66] Afzelius BA. Ultrastructure of human nasal epithelium during an episode of coronavirus infection. Virchows Arch 1994;424(3):295–300. doi:10.1007/bf00194614.

[67] Chen L, Li X, Chen M, Feng Y, Xiong C. The ACE2 expression in human heart indicates new potential mechanism of heart injury among patients infected with SARS-CoV-2. Cardiovasc Res 2020:cvaa078 [Epub ahead of print]. doi:10.1093/cvr/cvaa078.

[68] Madjid M, Vela D, Khalili-Tabrizi H, Casscells SW, Litovsky S. Systemic infections cause exaggerated local inflammation in atherosclerotic coronary arteries: clues to the triggering effect of acute infections on acute coronary syndromes. Tex Heart Inst J 2007;34(1):11–18.

[69] Wybraniec M, Mizia-Stec K, Krzych L. Stress cardiomyopathy: yet another type of neurocardiogenic injury: 'stress cardiomyopathy'. Cardiovasc Pathol 2014;23(3):113–20. doi:10.1016/j.carpath.2013.12.003.

[70] Ahmadjee A, Herzallah K, Saleh Y, Abela GS. Takotsubo Cardiomyopathy presenting with different morphological patterns in the same patient: a case report and review of the literature [published online ahead of print, 2020 Jan 15]. Cardiovasc Pathol 2020;47:107204. doi:10.1016/j.carpath.2020.107204.

[71] Aslam S, Mehra MR. COVID-19: yet another coronavirus challenge in transplantation. J Heart Lung Transplant 2020 S1053-2498(20)31468-6 [Epub ahead of print]. doi:10.1016/j.healun.2020.03.007.

[72] Vejpongsa P, Kitkungvan D, Madjid M, Charitakis K, Anderson HV, Arian S, et al. Outcomes of acute myocardial infarction in patients with influenza and other viral respiratory infections. Am J Med 2019;132(10):1173–81. doi:10.1016/j.amjmed.2019.05.002.

[73] Madjid M, Aboshady I, Awan I, Litovsky S, Casscells SW. Influenza and cardiovascular disease: is there a causal relationship? Tex Heart Inst J 2004;31(1):4–13.

[74] Li YC, Bai WZ, Hashikawa T. The neuroinvasive potential of SARS-CoV2 may play a role in the respiratory failure of COVID-19 patients. J Med Virol 2020 10.1002/jmv.25728 [Epub ahead of print]. doi:10.1002/jmv.25728.

[75] Paniz-Mondolfi A, Bryce C, Grimes Z, Gordon R, Reidy J, Lednicky J, et al. Central nervous system involvement by severe acute respiratory syndrome coronavirus -2 (SARS-CoV-2). J Med Virol 2020 10.1002/jmv.25915. doi:10.1002/jmv.25915.

[76] Oxley TJ, Mocco J, Majidi S, Kellner CP, Shoirah H, Sing P, et al. Large-vessel stroke as a presenting feature of Covid-19 in the young. N Engl J Med 2020 10.1056/NEJMc2009787. doi:10.1056/NEJMc2009787.

[77] Xu L, Liu J, Lu M, Yang D, Zheng X. Liver injury during highly pathogenic human coronavirus infections. Liver Int 2020 [Epub ahead of print]. doi:10.1111/liv.14435.

[78] Su H, Yang M, Wan C, Yi LX, Tang F, Zhu HY, et al. Renal histopathological analysis of 26 postmortem findings of patients with COVID-19 in China. Kidney Int. 2020. doi:10.1016/j.kint.2020.04.003.

[79] Pei G, Zhang Z, Peng J, Liu L, Zhang C, Yu C, et al. Renal involvement and early prognosis in patients with COVID- 19 pneumonia. J Am Soc Nephrol 2020 ASN.2020030276. doi:10.1681/ASN.2020030276.

[80] Cheng Y, Luo R, Wang K, Zhang M, Wang Z, Dong L, et al. Kidney disease is associated with in-hospital death ofpatients with COVID-19. Kidney Int 2020;97(5):829–38. doi:10.1016/j.kint.2020.03.005.

[81] Han M, Yan W, Huang Y, Yao H, Wang Z, Xi D, et al. The nucleocapsid protein of SARS-CoV induces transcription of hfgl2 prothrombinase gene dependent on C/EBP alpha. J Biochem 2008;144(1):51–62. doi:10.1093/jb/mvn042.

[82] Chang JC. TTP-like syndrome: novel concept and molecular pathogenesis of endotheliopathy-associated vascular microthrombotic disease. Thromb J 2018;16:20. doi:10.1186/s12959-018-0174-4.

[83] Chang JC. Sepsis and septic shock: endothelial molecular pathogenesis associated with vascular microthrombotic disease. Thromb J 2019;17:10. doi:10.1186/s12959-019-0198-4.

[84] Sarzi-Puttini P, Giorgi V, Sirotti S, Marotto D, Ardizzone A, Rizzardin G, et al. COVID-19, cytokines and immunosuppression: what can we learn from severe acute respiratory syndrome? Clin Exp Rheumatol 2020;38(2):337–42.

[85] Toh CH, Alhamdi Y, Abrams ST. Current pathological and laboratory considerations in the diagnosis of disseminated intravascular coagulation [published correction appears in Ann Lab Med. 2017 Jan;37(1):95]. Ann Lab Med 2016;36(6):505–12. doi:10.3343/alm.2016.36.6.505.

[86] Gorla R, Erbel R, Eagle KA, Bossone E. Systemic inflammatory response syndromes in the era of interventional cardiology. Vascul Pharmacol 2018 S1537-1891(18)30020-X [Epub ahead of print]. doi:10.1016/j.vph.2018.04.003.

[87] Varga Z, Flammer A.J., Steiger P., et al. Endothelial cell infection and endotheliitis in COVID-19. Lancet. doi:10.1016/S0140-6736(20)30937-5.

[88] Keller TT/, Mairuhu AT, de Kruif MD, Klein SK, Gerdes VEA, ten Cate H, et al. Infections and endothelial cells. Cardiovasc Res 2003;60(1):40–8. doi:10.1016/s0008-6363(03)00354-7.

[89] Singh S, Jindal AK, Pilania RK. Diagnosis of Kawasaki disease. Int J Rheum Dis 2018;21(1):36–44. doi:10.1111/1756- 185X.13224.

[90] Ascierto PA, Fox BA, Urba WJ, Bifulco CB, Botti G, Lugli A, et al. Insights from immuno-oncology: the Society for Immunotherapy of Cancer statement on access to IL-6-targeting therapies for COVID-19. J Immunotherap Cancer 2020 In press.

[91] Bikdeli B, Madhavan MV, Jimenez D, et al. COVID-19 and thrombotic or thromboembolic disease: implications for prevention, antithrombotic therapy, and follow-up. J Am Col Cardiol 2020. doi:10.1016/j.jacc.2020.04.031.

[92] Klok FA, Kruip MJHA, van der Meer NJM, Arbous MS, Gommers D, Kant KM, et al. Incidence of thrombotic complicationsin critically ill ICU patients with COVID-19. Thromb Res 2020 S0049-3848(20)30120-1. doi:10.1016/j.thromres.2020.04.013.

[93] Tang N, Bai H, Chen X, Gong J, Li D, Sun Z. Anticoagulant treatment is associated with decreased mortality in severe coronavirus disease 2019 patients with coagulopathy. J Thromb Haemost 2020 10.1111/jth.14817 [Epub ahead of print]. doi:10.1111/jth.14817.

[94] Thachil J. The versatile heparin in COVID-19. J Thromb Haemost 2020 10.1111/jth.14821 [Epub ahead of print]. doi:10.1111/jth.14821.

[95] Henry BM. COVID-19, ECMO, and lymphopenia: a word of caution. Lancet Respir Med 2020;8(4):e24. doi:10.1016/S2213-2600(20)30119-3.

[96] Fedson DS, Opal SM, Rordam OM. Hiding in plain sight: an approach to treating patients with severe COVID-19 infection. MBio 2020;11(2) e00398-20. Published 2020 Mar 20. doi:10.1128/mBio.00398-20.

[97] Patel AB, Verma A. COVID-19 and angiotensin-converting enzyme inhibitors and angiotensin receptor blockers: what is the rvidence? [published online ahead of print, 2020 Mar 24]. JAMA 2020 10.1001/jama.2020.4812. doi:10.1001/jama.2020.4812.

[98] Rossi GP, Sanga V, Barton M. Potential harmful effects of discontinuing ACE-inhibitors and ARBs in COVID-19 patients [published online ahead of print, 2020 Apr 6]. Elife 2020;9:e57278. doi:10.7554/eLife.57278.

[99] Menter T, Haslbauer JD, Nienhold R, Savic S, Hoper H, Deigendesch N, et al. Post-mortem examination of COVID19 patients reveals diffuse alveolar damage with severe capillary congestion and variegated findings of lungs and other organs suggesting vascular dysfunction. Histopathology 2020 10.1111/his.14134. doi:10.1111/his.14134.